Experimental Study on Pore Structure and Gas Desorption Characteristics of a Low Rank Coal: Impact of Moisture

Ming-yi Chen (chenmingyi@stdu.edu.cn)
Shijiazhuang Tiedao University
Ya-pu Yang
Shijiazhuang Tiedao University
Xiao-yun Chen
Shijiazhuang Tiedao University
Fu-chao Tian
China Coal Technology and Engineering Group Corp Shenyang Coal Research Institute
Wei-li Sun
China Coal Technology and Engineering Group Corp Shenyang Coal Research Institute
Yu-meng Yang
Shijiazhuang Tiedao University
Tong-hao Zhang
Shijiazhuang Tiedao University

Research

Keywords: Water adsorption, Pore structure, Fractal dimension, Methane desorption, Coal and gas outburst

Posted Date: December 8th, 2021

DOI: https://doi.org/10.21203/rs.3.rs-1110358/v1

Experimental study on pore structure and gas desorption characteristics of a Low rank coal: Impact of moisture

Chen Ming-yi[a,b,c]*, Yang Ya-pu[a,c], Chen Xiao-yun[a], Tian Fu-chao[d], Sun Wei-li[d], Yang Yu-meng[a,b,c], Zhang Tong-hao[a]

a School of safety engineering and emergency management, Shijiazhuang Tiedao University, Shijiazhuang 050043, China

b Hebei province technical innovation center of safe and effective mining of metal mines, Shijiazhuang Tiedao University, Shijiazhuang 050043, China

c Key Laboratory of Roads and Railway Engineering Safety Control (Shijiazhuang Tiedao University), Ministry of Education, shijiazhuang 050043, China

d State Key Laboratory of Coal Mine Safety Technology, China Coal Technology &Engineering Group Shenyang Research Institute, Shenfu Demonstration Zone 113122, China

***Corresponding author:** Chen Ming-yi

Address: School of safety engineering and emergency management, Shijiazhuang Tiedao University, Shijiazhuang 050043, China Tel.: +86 311 87936452 Fax: +86 311 87936452

E-mail address:

Chen Ming-yi chenmingyi@stdu.edu.cn

Yang Ya-pu yangyapu97@163.com

Chen Xiao-yun chenxiaoyun18@126.com

Tian Fu-chao tianfuchao@cumt.edu.cn

Sun Wei-li vealy_sun1989@163.com

Yang Yu-meng aqyangyumeng@stdu.edu.cn

Zhang Tong-hao zth15732169205@163.com

Abstracts: Coal and gas outburst is one of the most serious disasters for underground coal mining. The water adsorbed on coal can leads to that the pore structure of moist coal is different from that of dry coal, thereby affecting methane desorption characteristics of coal for the outburst risk prediction. In this paper, the impact of moisture on pore structure and methane desorption performance were investigated. The analysis on low-temperature nitrogen gas adsorption tests show that the micropores (pore diameter < 10 nm) are most affected by the adsorbed water. In particular, for water-equilibrated coal sample at 98% relatively humidity, the micropores less than 4 nm analyzed by DFT pore size distributions almost disappear probably due to the blocking effect of the formed water clusters and capillary water. In this case, the micropores can still contributes most sites for gas adsorption. Furthermore, the fractal dimension at relative pressure of 0–0.5 (D_1) and 0.5–1 (D_2) calculated by the Frenkel-Halsey-Hill model indicates that, when moisture content is less than 4.74%, D_1 decreases rapidly while D_2 shows a slight change; whereas, further increases in moisture content results in that D_2 decreases significantly and D_1 remains at about 2.32. Further investigation shows that, below the equilibrium moisture content, the ultimate desorption volume (A) and initial desorption rate (V_0) are closely related to D_1, while the desorption constant (K_t) mainly depends on D_2. Therefore, the adsorbed moisture has significant negative impact on methane desorption performances by affecting characteristics of coal's pores.

Keywords: Water adsorption; Pore structure; Fractal dimension; Methane desorption; Coal and gas outburst

1 Introduction

Currently, although the casualties caused by coal mine disasters have been effectively controlled, coal and gas outburst is still one of the most serious disasters associated with coal mine (Fu et al. 2020; Wang et al. 2014b; Zhai et al. 2016). A coal and gas outburst is closely related to the methane

desorption capacity of coal, and many methane desorption indices are used to predict the outburst risk (Wang et al. 2020b; Xue et al. 2020). Therefore, understanding the methane desorption characteristics of coal is critical for the prediction of coal and gas outburst. Coal is a porous medium with a highly developed pore system (Cheng and Pan 2020; Lu et al. 2021). Water in coal can be divided into two types: inherent moisture in coal matrix and free water in cleat system (Pan et al. 2010). The inherent moisture mainly exists in the absorbed state, which can occupy the surface sites of coal pores due to the physical adsorption and oxygen-containing functional group effects (Wang et al. 2021). Moreover, the existing of oxygen-containing functional groups (e.g. carboxylic and hydroxyl groups) adsorption sites are preferably occupied by water molecules (Li et al. 2019). Therefore, the adsorption advantage of water molecules will weaken the capacity of coal adsorbing gas, thereby affecting desorption and migration of methane gas in coal body.

Many scholars have long been concerned about moisture influences on gas adsorption and desorption of coal through experimental, numerical simulation and mathematical theory methods. The existence of water can significantly reduce the methane adsorption capacity of coal (Busch and Gensterblum 2011; Nie et al. 2016), which is mainly due to the competitive adsorption of water and methane and the advantage of coal adsorbing water molecules (Gensterblum et al. 2014; Xiang et al. 2014). It has been reported that 2% moisture content can result in an approximately 20% reduction in both CH_4 and CO_2 adsorption capacity of moist coal (Clarkson and Bustin 2000). The impact of water on methane adsorption capacity is also related to the metamorphic degree of coal. Dry coal shows a trend of first falling and then rising with increasing coal rank, whereas the methane adsorption capacity of the water-equilibrated coal increases slightly with coal rank (Laxminarayana and Crosdale 2002). It is further found that the adsorbed water can induces the reduction in methane adsorption capacity of a

bituminous coal and the non-adsorbed water has no effect; in contrast, for anthracite coal, both the two form of water have remarkably weaken on methane adsorption, which is considered to be related to the difference in pore structure between the two coal samples (Wang et al. 2020a). Besides, water also has great weakening impact on methane desorption and diffusion capacities of coal (Liu et al. 2019; Pan et al. 2010). Combined with unipore, bidisperse and other diffusion models, it is observed that increasing moisture content causes both micropores and macropores diffusion coefficients to decrease for different rank coals (Guo et al. 2018; Wang et al. 2017). Other studies further show that increasing equilibrium moisture content can induces the continual decreases in diffusivity for anthracite coal and the U-shaped change in diffusivity for bituminous coal. This may be caused by the different moisture effects between the reduction in adsorbed gas volume and the decrease of pore space for various rank coals (Wang et al. 2014a). Furthermore, increasing moisture content can also decreases the methane desorption volume and velocity of coal, which has been widely accepted by scholars (Chen and Cheng 2015; Meng et al. 2020; Zhang et al. 2018).

Generally, coal with $R_{o,max}$ less than 0.65% is classified as low-rank coal in China (Wang et al. 2017), which includes lignite and some long-flame coal. Low-rank coal generally features a higher adsorbed water content than middle-high rank coals, because low-rank coal has a larger porosity, specific surface area (SSA) and more oxygen-containing functional groups (Chen et al. 2018; Yu et al. 2013). Statistics show that in China, the moisture content of lignite is 10–28% and that of long-flame coal mostly is 3–12% (Guo et al. 2015). Hence, more studies on the influence of adsorbed water on the methane desorption characteristics of low-rank coal are needed.

In this paper, a typical long-flame coal was used to perform the following studies: (1) water adsorption characteristics of coal and pore structure of water-equilibrated coal at different relatively

67 humidity, (2) the relationships between adsorbed moisture content and fractal dimension of coal pores,
68 (3) the impact of adsorbed moisture on methane desorption performances and its relations with fractal
69 dimension.

70 **2 Experiment and method**

71 **2.1 Coal preparation and Basic parameters**

72 *2.1.1 Basic parameters*

73 The low rank coal sample was selected from the No. 2 coal seam in the Yuanzigou coal mine,
74 Baoji city, Shaanxi Province. The geological survey data show that the moisture content of the No. 2
75 coal seam on air dry basis is 3.60–11.28%. Several kilograms of fresh lump coal were collected from
76 the working face, and various sizes of coal particles were prepared by crushing and screening.
77 Following the ISO 17246:2010 standard, the coal sample with sizes of 0.074–0.20 mm was selected to
78 perform the proximate analysis by an automatic proximate analyzer. The vitrinite reflectance of coal
79 reflects the coalification degree, which was determined by following the ISO 7404–5:2009 standard.
80 The ash content on air dry basis (A_{ad}), volatile matter on dry ash free basis (V_{daf}), fixed carbon on air
81 dry basis (FC_{ad}), maximum vitrinite reflectance ($R_{o,\,max}$) are shown in Table 1.

82 **Table 1 Basic parameters of coal sample.**

Sample	$R_{o,max}$/%	M_{ad}/%	A_{ad}/%	V_{daf}/%	FC_{ad}/%
Long-flame coal	0.65	6.33	26.59	40.53	39.90

83 *2.1.2 Preparation of moist coal samples*

84 First, the coal samples with particle sizes of 0.2–0.25 mm were placed in a vacuum drying oven at
85 378 K for at least 8 h to remove the original moisture. Eight saturated salt solutions were selected to
86 prepare the water-equilibrated coal sample under a constant relatively humidity (*RH*) condition. The
87 *RH* was 11% for LiCl, 23% for CH_3COOK, 33% for $MgCl_2$, 43% for K_2CO_3, 57% for NaBr, 75% for
88 NaCl, 85% for KCl, and 98% for K_2SO_4 at a room temperature of 293 K. Approximately 5 g of coal

sample was placed into glassware containing saturated salt solution, and the glassware was sealed with vacuum silica gel. A high-precision electronic balance (FA2204) was used to weigh the coal samples at 8 h intervals. When the quality of the sample remains steady, it was considered that the water adsorption equilibrium was achieved under the corresponding relative humidity (*RH*) conditions. Subsequently, the moisture content of the coal sample under different *RH* conditions was calculated by the following equation:

$$M = \frac{(m_{moist} - m_{dry})}{m_{dry}} \quad (1)$$

Where M is the moisture content, %; m_{moist} is the weight of moist sample at a certain *RH*, g; and m_{dry} is the weight of dry sample, g. The water adsorption test was repeated twice and the mean values of moisture content at different relative humidity were determined for further study.

Furthermore, the water adsorption characteristic of the studied coal was analyzed by a modified Guggenheim–Anderson–de Boer (M-GAB) model. The M-GAB model is based on the BET and GAB model, which has been proved to be a good characterization of water vapor adsorption on porous materials (Zou et al. 2016). The M-GAB model, like GAB and M-Dent model (Duan and Li 2018), assumes water molecules adsorb on two sites: primary adsorption sites and secondary adsorption sites and one molecule occupies α sites when being adsorbed. The M-GAB model can be described by the following equation:

$$M = \frac{M_0 * C * K * x^{\alpha}}{(1 - K * x^{\alpha})(1 - K * x^{\alpha} + C * K * x^{\alpha})} \quad (2)$$

Where M_0 is the monolayer adsorption capacity, x is relative humidity, C and K are the adsorption constants related to primary sites and secondary sites, respectively, and α represents the heterogeneity of the adsorption system. The water adsorption amounts of primary and secondary sites have the following relationships (Andrade et al., 2011):

$$M_1 = \frac{M_0*(C-1)*K*x^{\alpha}}{1-K*x^{\alpha}+C*K*x^{\alpha}} \quad (3)$$

$$M_2 = \frac{M_0*K*x^{\alpha}}{1-K*x^{\alpha}} \quad (4)$$

2.2 Low-temperature nitrogen gas adsorption test

Low-temperature nitrogen gas adsorption (LN_2GA) was an important physical method to characterize the nanopores of porous media. In this study, the test instrument was an Autosorb-iQ2 analyzer (Quantachrome Ins, USA). The N_2 ad/desorption isotherms at a P/P_0 of 0.001–0.995 of coal samples were measured. Before the LN_2GA tests, according to the moist coal sample preparation processes in Section 2.1.2, the coal samples with different water content were prepared. Then, the moist coal samples were placed in liquid N_2 environments at a temperature of ~77 K for several minutes. Under these conditions, the moist samples were frozen so that the loss of pre-adsorbed water could be ignored. At the same time, the vacuum pumping step was omitted to avoid the loss of water in the tested samples.

2.3 Tests and Analytical methods for methane desorption in coal

2.3.1 Methane desorption tests

The bulk desorption method (Zhang 2008) was applied to perform the methane desorption test of coal samples with particle sizes of 0.2–0.25 mm. First, approximately 50 g of coal sample was put into a coal sample tank. To reduce the loss of water from the coal sample as much as possible, the vacuum pumping time was operated for no longer than 30 min. Then, the methane gas with a purity of 99.99% was pumped into the coal sample tank to a gas pressure, and the coal sample tank was put into a stable temperature water bath at 303.15 K. Subsequently, the gas pressure of the coal sample tank was adjusted to a predetermined pressure (1 MPa). When the pressure gauge remained constant for 8 h, it is deemed that the gas-containing coal sample has achieved the adsorption equilibrium state. Finally, the

133 free gas of the coal sample tank was removed, and then a methane desorption test of coal sample can be
134 performed. The test time was conducted for 120 min, and the methane desorption volume of coal at
135 regular intervals and the ultimate desorption volume (Q_∞) were recorded. The moisture content of the
136 test sample was measured by the weighing method after the methane desorption test.

137 *2.3.2 Analytical methods of desorption data*

138 Currently, numerous of mathematical equations have been proposed to describe the gas desorption
139 law of coal particles (Cheng et al. 2010). Among them, the Airey-type and Winter-type equations are
140 often used to analyze the law of underground coal seam gas desorption and emission.

141 Airey believed that the coal body could be regarded as a material composed of separated blocks
142 containing fractures and proposing the following formula (Airey 1968):

143 $$Q_t = A\left[1 - exp\left\{-\left(\frac{t}{t_0}\right)^n\right\}\right] \quad (5)$$

144 where Q_t is the gas desorption volume at time t, cm^3/g; A is the ultimate desorption volume,
145 cm^3/g; t_0 is the desorption time constant; and n is a coefficient.

146 In Winter's theory, when the gas pressure was removed, the change in the gas desorption rate with
147 time can be described by the following power function (Winter and Janas 1975):

148 $$V_t = V_a\left(\frac{t}{t_a}\right)^{-K_t} \quad (6)$$

149 After mathematical integration, the relationship between methane desorption volume and time can
150 be obtained, as shown in the following equation:

151 $$Q_t = \frac{V_1}{1-K_t}t^{1-K_t} \quad (7)$$

152 where Q_t is the cumulative desorption volume at time t, cm^3/g; V_1 and V_a are the methane
153 desorption rates at times t_1 and t_a, respectively, cm^3/(g·min); and k_t is a constant that reflects the degree
154 of attenuation of the desorption rate (Banerjee 1988).

3 Experimental results

3.1 Water adsorption isotherms

The M-GAB model fitting for water adsorption data of the studied coal sample is shown in Figure 1. According to the International Union of Pure and Applied Chemistry (IUPAC) classification (Lowell et al. 2004), the adsorption curve belongs to type II isotherms. The M-GAB model has excellent fitting effect with a R^2 value of 0.9975. The water adsorption amount shows stage characteristics. Under the conditions of RH< 0.2 and RH> 0.8, the water adsorption amount increases rapidly. When RH ranges from 0.2 to 0.8, the growth of water adsorption capacity is relatively gentle.

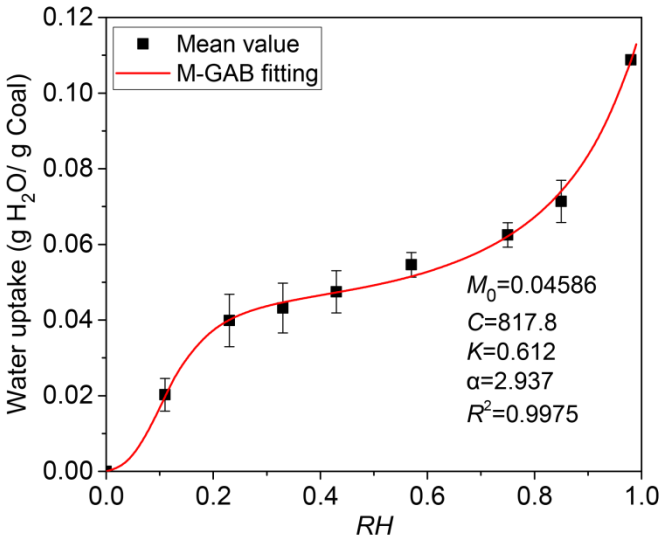

Figure 1 The M-GAB model fitting for water adsorption of the studied sample.

3.2 LN_2GA isotherms

The LN_2GA adsorption and desorption isotherms of coal samples are illustrated in Figure 2. The adsorption isotherms of dry and moist samples belong to type II of the IUPAC classification. With the moisture content increases, the slope of nitrogen adsorption curve decreases at the pressure range of 0.1 to 0.9. For the maximum nitrogen adsorption amount, the dry coal sample is 20.24 cm^3/g, whereas, that of water-equilibrated coal sample at 98% RH (M= 10.88%) is reduced by nearly 50%. In the low relative pressure range (P/P_0<0.01), the nitrogen adsorption capacity of coal samples generally

increases significantly, which is mainly related to the micropores filling effect caused by a large number of micropores in coal (Hong et al. 2019; Kondo et al. 2005). It can be observed that the nitrogen adsorption curves at $P/P_0 < 0.1$ become flatter with increasing moisture content, which reflects that the micropores filling effect is weakened for gas adsorption on moist coal samples. When the P/P_0 is close to 1.0, all adsorption curves increase sharply, which indicates that water has a weak impact on nitrogen gas adsorption in larger scale pores of coal.

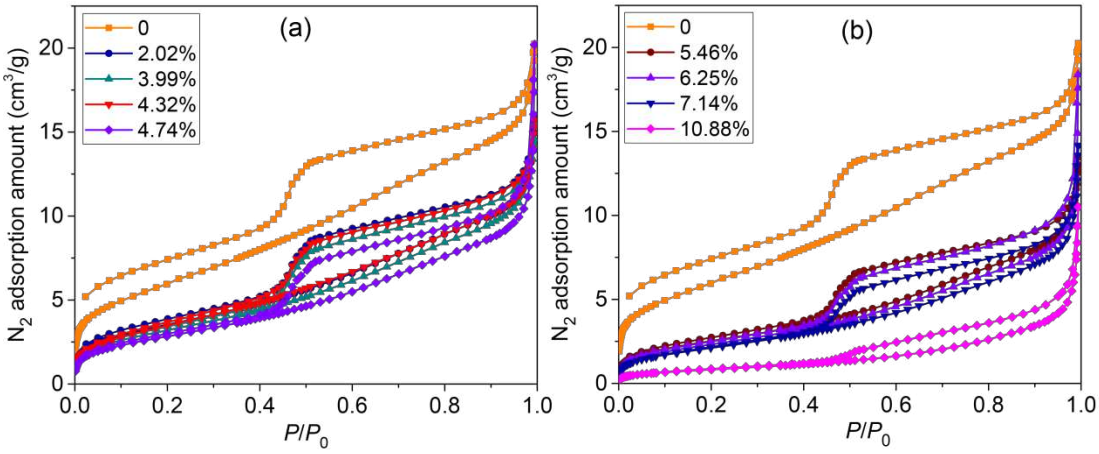

Figure 2 Low-temperature nitrogen ad/desorption isotherms of coal samples.

In addition, all coal samples show a prominent adsorption hysteresis characteristics, the features of the hysteresis loop correspond to types H3 and H4 in the IUPAC classification (Thommes et al. 2015), and its size tends to decrease with increasing moisture content. The coal samples with moisture content less than 7.14% (corresponding to *RH* of 85%) exhibit an inflection point of the desorption curve at the P/P_0 around 0.45, which is considered to be related to the existence of ink-bottle pores (Liu et al. 2021; Qi et al. 2017). The desorption curve of coal sample around the inflection point gradually shrinks with moisture content increases. When the moisture content increases to the maximum equilibrium moisture content (10.88%), the inflection point of desorption curve almost disappears.

3.3 Methane desorption characteristics

For the methane desorption isotherms at gas pressure of 1 MPa, the fit curves of the Winter-type

and Airey-type equations are shown in Figure 3. The desorption process can be divided into rapid growth period (①), stable growth period (②) and slow growth period (③). It can be observed that the cumulative desorption amount shows a monotonous upward trend of the parabola with increasing desorption time. Besides, the cumulative desorption amount of coal samples decreases with the moisture content increases.

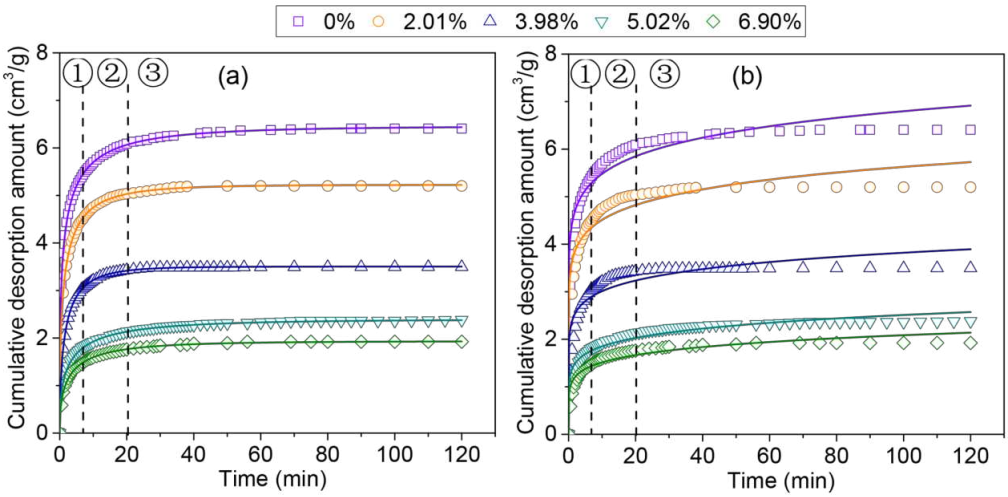

Figure 3 Methane desorption data and fit curves of coal samples at methane pressure of 1 MPa; (a) Airey-type fit; (b) Winter-type fit.

The fit results of the Airey-type and Winter-type equations are shown in Table 2. The correlation coefficient R^2 of the Airey-type equation is 0.9989–0.9998; for the Winter-type equation, it is 0.8670–0.9373. The Airey-type equation exhibits a higher fit accuracy than the Winter-type equation. The parameters A and V_1 represent the ultimate methane desorption capacity and the initial rate of methane desorption, respectively (Chen et al. 2017; Guo et al. 2018). Obviously, increasing the moisture content can causes a significant reduction in methane desorption capacity.

Table 2 Fitting results of the tested samples by Airey-type and Winter-type equations

Moisture content /%	Airey's equation				Winter's equation		
	A /(cm³/g)	t_0 /min	n	R^2	V_1 /(cm³/(g·min))	k_t	R^2
0	6.460	1.406	0.387	0.9998	0.413	0.907	0.9373
2.01	5.225	1.530	0.463	0.9997	0.347	0.904	0.9013
3.98	3.504	1.901	0.554	0.9997	0.245	0.897	0.8670
5.02	2.392	3.329	0.446	0.9989	0.180	0.868	0.9290
6.90	1.934	3.175	0.484	0.9989	0.153	0.861	0.9139

205 Furthermore, the methane desorption amounts at different periods are illustrated in Table 3. The
206 methane desorption volume of coal in the first minute (Q_1) and the third to fifth minute ($Q_{3\text{-}5}$) are two
207 important parameters for predicting the risk of coal and gas outburst of a coal seam (Cheng et al. 2010).
208 The errors of parameter A are 0.22–0.85% for methane pressure of 1 MPa, so parameter A is very close
209 to the measured value Q_∞. Therefore, the Airey-type equation is more suitable to describe the methane
210 desorption behavior of coal.

211 **Table 3 Results of methane desorption amounts in different desorption periods.**

Moisture content /%	Q_1 /(cm^3/g)	$Q_{3\sim5}$ /(cm^3/g)	Q_∞ /(cm^3/g)	$\left\|\frac{A-Q_\infty}{Q_\infty}\right\|$ (%)
0	3.791	0.413	6.406	0.85
2.01	2.950	0.405	5.199	0.50
3.98	1.778	0.325	3.496	0.22
5.02	1.018	0.177	2.380	0.54
6.90	0.857	0.172	1.922	0.63

212 **4 Analysis and Discussion**

213 **4.1 Water adsorption behavior of coal**

214 The water adsorption isotherms of primary sites and secondary sites calculated by the M-GAB
215 model for the studied coal sample are plotted in Figure 4. The initial water adsorption amount is mainly
216 contributed by the primary sites, and the primary sites adsorption isotherms coincides with type I in the
217 IUPAC classification (Lowell et al. 2004), which signifies that the primary sites adsorption is confined
218 to a monolayer. With increasing relative humidity, the secondary sites adsorption becomes crucial, and
219 the secondary sites adsorption corresponds to the type III isotherms associated with multilayer
220 adsorption. An inflection point around *RH* of 0.2 can be observed in the M-GAB fitting curve,
221 indicating the completion of monolayer coverage and the beginning of multilayer adsorption
222 (Thommes et al. 2015). When the *RH* exceeds 0.5, the primary adsorption approach the dotted line
223 representing the amount of saturated monolayer adsorption (M_0) calculated by the M-GAB model, and

224 then the water clusters gradually form (Charrière and Behra 2010). As the *RH* increases, the water
225 uptake increases sharply at the region of *RH* > 0.8, which is related to the capillary condenstation of
226 water in pores.

227 Besides, in the M-GAB model, *C* relates to adsorption energies of water molecules on primary
228 sites, while *K* associates with adsorption energies of the interaction between water molecules and
229 adsorbed water molecules at secondary sites (Zou et al. 2016). For the studied coal sample, the value of
230 *C* is far larger than that of *K*, which is mainly due to that the weak interactions of coal-water molecules
231 need more energy than the strong interactions of water-water molecules (Duan and Li 2018; Charrière
232 and Behra 2010).

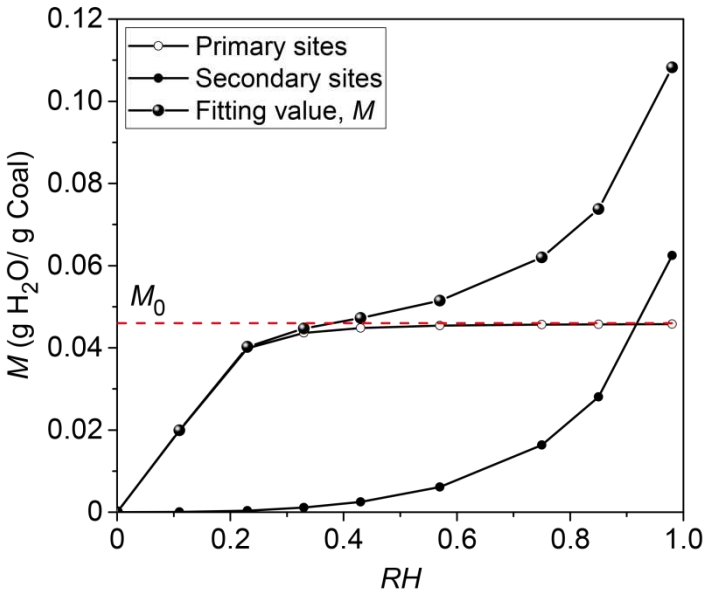

233

234 Figure 4. Amount of water adsorption on primary sites and secondary sites.

235 **4.2 Impact of water on pore structure of coal**

236 *4.2.1 N_2-SSA and N_2-PV*

237 The pore size classification method proposed by B.B. ХОДОТ has widely used, and coal pores are
238 divided into five categories (Chen et al. 2015; Jiang et al. 2016). Among them, micropores (d<10 nm)
239 constitutes gas adsorption volume of coal, transition pores (10<d<100 nm) is the gas diffusion space,

240 The pore diameter of 100 nm is always considered to be a cut point for gas diffusion and seepage
241 (Chen et al., 2017), and mesopores (100<*d*<1000 nm) forms a slow seepage space. In this paper, after
242 integrating the pore parameters from the QSDFT model (1–10 nm) and BJH model (10–300 nm), the
243 specific surface area (SSA), pore volume (PV) of different scales pores (micropores, transition pores,
244 mesopores) are calculated, as illustrated in Table 4. When the moisture content increases to the
245 equilibrium moisture content of 2.02% (corresponding to *RH* of 11%), the total SSA can be decreased
246 by about 39.3%. With increasing moisture content, both the total SSA and total PV tend to decrease,
247 whereas the average pore diameter (PD) shows an increase tendency. For the water-equilibrated coal
248 sample at 98% *RH* (*M* = 10.88%), the total SSA and total PV were reduced to 16.31% and 53.47%,
249 respectively. That indicates that the adsorbed water can leads to a significant reduction in the SSA of
250 coal.

251 **Table 5 Pore parameters of coal samples from LN_2GA tests.**

Sample no.	Mean moisture content (%)	SSA (m^2/g)				PV ($\times10^{-3}cm^3/g$)				PD (nm)
		S1	S2	S3	Total	V1	V2	V3	Total	
YZG1	0	16.44	1.12	0.096	17.66	18.79	7.20	4.83	30.82	5.66
YZG2	2.02	9.59	1.02	0.101	10.71	12.52	6.86	4.91	24.28	7.51
YZG3	3.99	8.72	1.03	0.096	9.85	11.75	6.98	5.09	23.82	7.97
YZG4	4.32	9.47	1.01	0.098	10.57	12.52	6.76	4.84	24.12	7.29
YZG5	4.74	7.68	1.01	0.24	8.93	10.53	7.26	13.50	31.29	11.63
YZG6	5.46	6.80	0.96	0.094	7.85	9.55	6.50	4.74	20.79	8.88
YZG7	6.25	6.23	0.99	0.21	7.43	8.91	7.33	10.98	27.23	12.38
YZG8	7.14	5.65	0.96	0.13	6.73	8.20	6.84	6.80	21.84	10.81
YZG9	10.88	1.95	0.79	0.14	2.87	3.35	5.94	7.19	16.48	20.50

252 Note: Si (Vi) represents the SSA and PV of micropores, transition pores and mesopores, respectively, where i= 1, 2, 3.

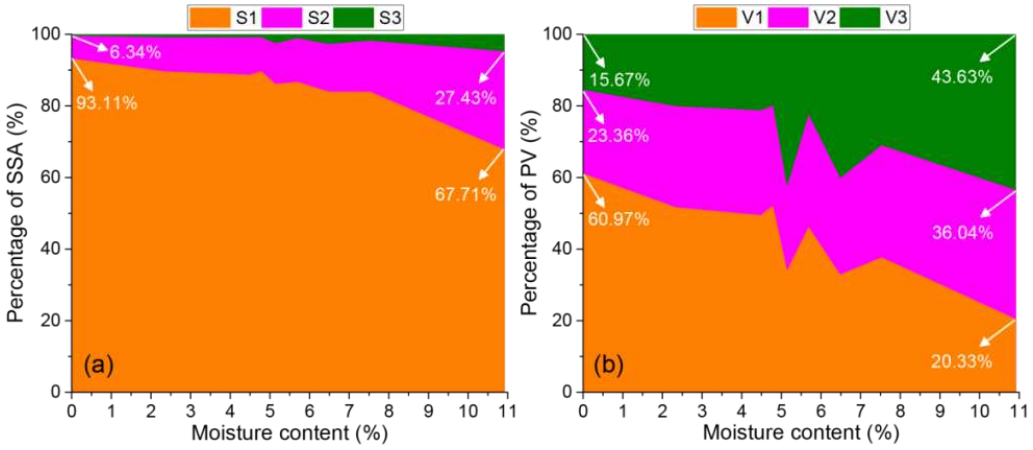

Figure 5. Change in percentage of SSA and PV of different scale pores with moisture content.

The percentages of SSA and PV of different scale pores (micropores, transition pores, mesopores) are shown in Figure 5. The micropores SSA of sample YZG1 accounts for 93.11%, which indicates that the micropores plays a key role in gas adsorption at dry condition. The percentage of micropores SSA shows a decreasing trend with increasing moisture content, and that of sample YZG9 decreased to the lowest value (67.71%). This means that the micropores can still contribute most sites for nitrogen adsorption on water-equilibrated coal samples. For pore volume, with increasing moisture content, the percentage of micropores volume also shows a decreasing trend, and 60.97% is for sample YZG1 at dry condition and only 20.33 % is for sample YZG9 that is attained at water-equilibrated condition of 98% *RH*. In contrast, the percentage of SSA and PV of both transition pores and mesopores show an increasing trend. Therefore, water can significantly reduce the SSA and PV of coal pores. In particular, the micropores (d<10 nm) are most significantly weakened owing to the existence of water.

4.2.2 Pore size distribution

Thommes et al. (2015) indicated that the BJH method is more suitable for pore size analysis of mesopores and larger pores (>10 nm), and the DFT method can provides a reasonably reliable assessment of the nanopore size distributions. In this paper, both DFT and BJH models are employed to investigate the PSDs (pore size distributions) of pores with the size of 1–300 nm. The BJH-PSDs

curves of the coal samples are illustrated in Figure 6. All samples show multi-peak distribution characteristics, and there are a large number of nanopores in the size range of 3–300 nm. With increasing moisture content, the dV(d) value of coal samples gradually approach the X-axis, especially for micropores (d<10 nm). The DFT-PSDs curves of coal samples are shown in Figure 7. The DFT dV(d) plots of coal samples with moisture content less than 7.14% mainly exhibit bi-peak values at ~1.1 nm and ~5.0 nm, whereas, that of sample YZG9 (M= 10.88%) shows an uni-peak at ~5.6 nm. The DFT dV(d) value tends to decrease with increasing moisture content, and when the moisture content reaches 10.88%, the peak value of dV(d) approaches 0 at ~1.1 nm, thereby indicating that pores less than 4 nm almost disappear for water-equilibrated coal sample YZG9. For both DFT-PSDs and BJH-PSDs curves, there is no significant difference in the PSDs of pores greater than 10 nm for coal samples with different moisture content. Therefore, water mainly has a significant impact on micropores (d< 10 nm) of coal, which can be attributed to the adsorption of water on coal surface. Under the condition of low moisture content, the effective sites for CH_4 or N_2 molecules are decreased by the preferential adsorption of water molecules (Gensterblum et al. 2014; Gensterblum et al. 2013). With a further increase in moisture content, the multilayer adsorption will occurs and the thickness of water molecule layers becomes significant. The process can results in the formation of water clusters (Do and Do, 2009; Charrière and Behra, 2010). And further the growth of water clusters and the capillary condensation will fill up some small pores. With a further increase in *RH*, the adsorbed moisture content of coal is enhanced (Figure 1). Especially for the water-equilibrated coal sample YZG9 at 98% *RH*, some pore throats can be blocked by the adsorbed water, thereby hindering the intrusion of gas molecules into the micropores. Thus the available nanopores for methane molecules adsorption on the water-equilibrated coal at 98% *RH* are mainly larger-scale pores (pore diameter > 4

nm).

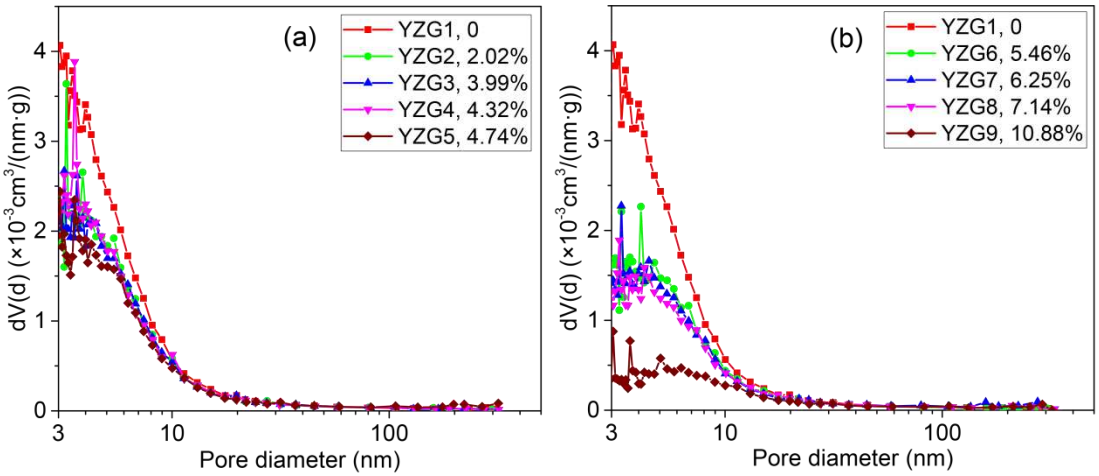

Figure 6 BJH-PSDs curves of coal samples.

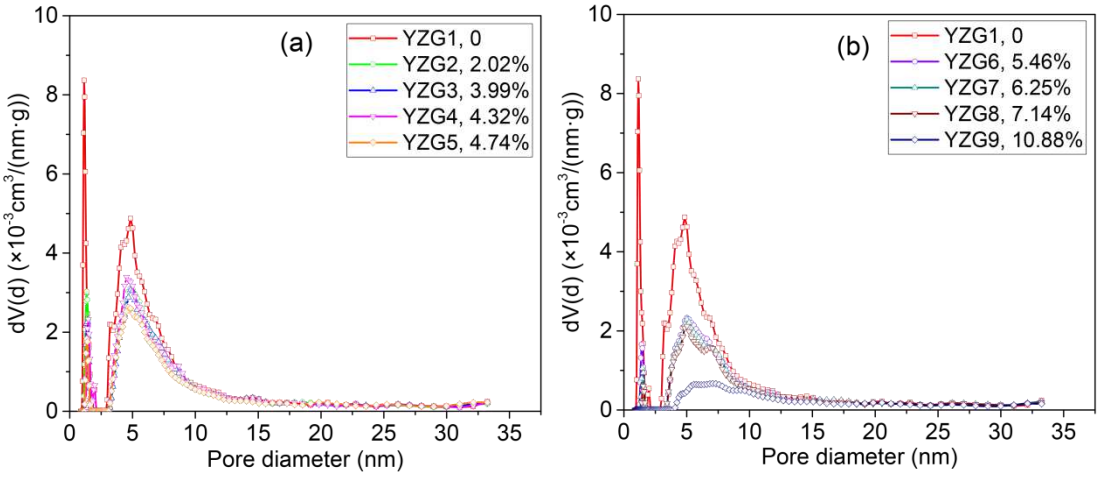

Figure 7 DFT-PSDs curves of coal samples.

4.3 Fractal characteristics of coal pores under moist condition

Based on the LN_2GA data, the fractal dimension can be determined by the fractal Frenkel-Halsey-Hill (FHH) equation (Ni et al. 2020; Si et al. 2021; Liu and Nie 2016). It can be described by the following expression:

$$\ln V = A\left[ln ln(\frac{P_0}{P})\right] + B \quad (8)$$

Where V is the gas adsorption amount at adsorption equilibrium pressure P; P_0 is the saturated gas pressure; A is the slope of the fitting line, which is linear with the fractal dimension D, and there are two mathematical expressions for A and D, namely, A=D–3 and A=(D–3)/3; and B is a constant. The

306 fractal dimension, D ranges from 2 to 3, which can reflects the irregularity of coal pores. The closer D
307 is to 2, the smoother the pore surface is; and the closer D is to 3, the more complex the pore surface is.
308 Low-temperature nitrogen desorption isotherms is generally used to calculate the fractal
309 dimension, because the corresponding adsorption state is more stable (Li et al. 2015). In the region of
310 $P/P_0 < 0.5$, the adsorption and desorption curves essentially parallel and even coincide, while in the
311 region of $P/P_0 > 0.5$, there is significant adsorption hysteresis. This phenomenon suggests that the
312 mechanisms of coal adsorbing gas are different for the two pressure regions. The fractal dimension of
313 the two regions is always calculated with the relative pressure of 0.5 as the dividing point (Yao et al.
314 2008). The results of the fractal dimension D calculated by the FHH equation are illustrated in Table 5.
315 The calculation results obtained by the equation '$A=D-3$' are between 2 and 3, which is more
316 reasonable than the calculation from the equation '$A=(D-3)/3$'. It can be seen that D_1 is 2.296–2.534
317 and D_2 is 2.651–2.912.

318 Table 5 The fractal dimensions calculated by FHH model for low-temperature nitrogen desorption
319 isotherms.

Sample no.	Mean moisture content/%	A_1	$D_1=3+A_1$	$D_1=3+3A_1$	R^2	A_2	$D_2=3+A_2$	$D_2=3+3A_2$	R^2
YZG1	0	-0.466	2.534	1.602	0.9533	-0.088	2.912	2.737	0.9769
YZG2	2.02	-0.617	2.383	1.149	0.9594	-0.123	2.877	2.632	0.9604
YZG3	3.99	-0.687	2.313	0.938	0.9543	-0.134	2.866	2.599	0.9695
YZG4	4.32	-0.704	2.296	0.888	0.9649	-0.127	2.873	2.619	0.9737
YZG5	4.74	-0.667	2.333	0.998	0.9605	-0.193	2.807	2.421	0.9586
YZG6	5.46	-0.666	2.335	1.004	0.9561	-0.147	2.853	2.558	0.9575
YZG7	6.25	-0.677	2.323	0.970	0.9629	-0.216	2.784	2.351	0.9638
YZG8	7.14	-0.694	2.306	0.919	0.9826	-0.196	2.804	2.412	0.9471
YZG9	10.88	-0.666	2.334	1.003	0.9914	-0.349	2.651	1.952	0.9360

320 The relationships between the fractal dimensions D_1, D_2 and moisture content are shown in Figure
321 8. When the moisture content is less than 4.74% (corresponding to RH of 43%), D_1 decreases rapidly,
322 whereas D_2 reduces from 2.91 to 2.87, showing a slight change. When the moisture content increases
323 from 4.74% to 10.88% (corresponding to RH of 98%), D_2 decreases significantly, while D_1 remains at

about 2.32.

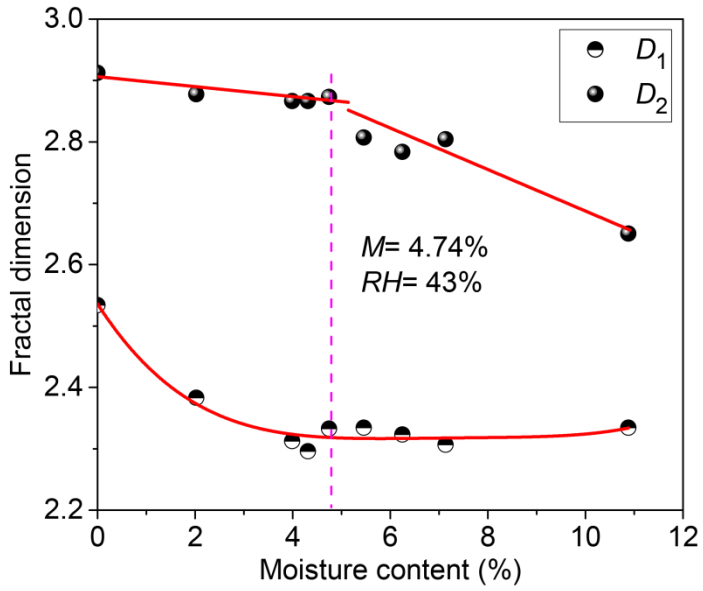

Figure 8 Relationships between fractal dimensions D_1 and D_2 and moisture content.

Water sorption on coal is gradually divided into the following stages (Liu et al. 2020): primary adsorption, secondary and even multilayer adsorption, the formation of water clusters, and capillary condensation of water. As illustrated in the section 4.1, when the *RH* is lower than 43% (corresponding of equilibrium moisture content of 4.74%), the adsorbed water content shows a Langmuir-type trend with an increase in *RH*, indicating that the water adsorption on coal mainly occurs on the primary sites, i.e., oxygen-containing functional groups (Charrière and Behra 2010; Švábová et al. 2011). In this process, water molecules are preferentially adsorbed on the surface of micropores, which can result in that the homogeneity of surface of micropores is enhanced for the water-equilibrated coal. This should be responsible for the significant reduction of fractal dimension D_1. As the relative humidity increases ($RH > 43\%$), the secondary sites adsorption gradually turns into the main behavior. In this process, the formed water clusters grow continuously and capillary condensation will occurs. As shown in Figures 6 and 7, the PSDs curves of micropores shrinks close to the X-axis, while these of larger scale pores (pore diameter > 10 nm) is basically unchanged. This shows that the water molecules adsorbing on the

larger scale pores fails to cause a significant variation in the nitrogen molecules on the surface of larger scale pores. However, the formed water clusters and capillary water will occupy the pore space and even fill some small pores and throat, thereby improving the homogeneity of pores structure. These should be responsible for the reduction in fractal dimension D_2 at high equilibrium moisture content (M > 4.74%). However, in the same stage, the fractal dimension D_1 is basically unchanged, which may be related to (i) the completion of saturated monolayer adsorption of water molecules on micropores; and (ii) the inability of gas molecules to pass through the pores and throat blocked by the adsorbed water.

4.4 Impact of moisture on methane desorption performances

4.4.1 Methane desorption characteristics of moist coals

The parameters K_1, Δh_2 are always selected as the methane desorption indices to predict the outburst risk of mining coal seams (Cheng et al. 2010). The two indices reflect the methane desorption performances of coal samples in the first minute (Q_1) and the third to fifth minutes ($Q_{3\text{-}5}$) (Chen and Cheng 2015; Jiang et al. 2015). The relationships between the initial desorption amounts Q_1 and $Q_{3\text{-}5}$ and moisture content are shown in Figure 9. The two desorption parameters decrease with moisture content in negative exponential form. In the range of the studied moisture content, the parameters Q_1 and $Q_{3\text{-}5}$ are reduced by 77.39% and 58.35%. Namely, each 1% increase in moisture content can leads to about 11% reduction in Q_1 and about 8% reduction in $Q_{3\text{-}5}$, respectively. Therefore, moisture has a weakening effect on the initial methane desorption capacity of coal, and Q_1 (corresponding to K_1 index) is more significantly affected than $Q_{3\text{-}5}$ (corresponding to Δh_2 index).

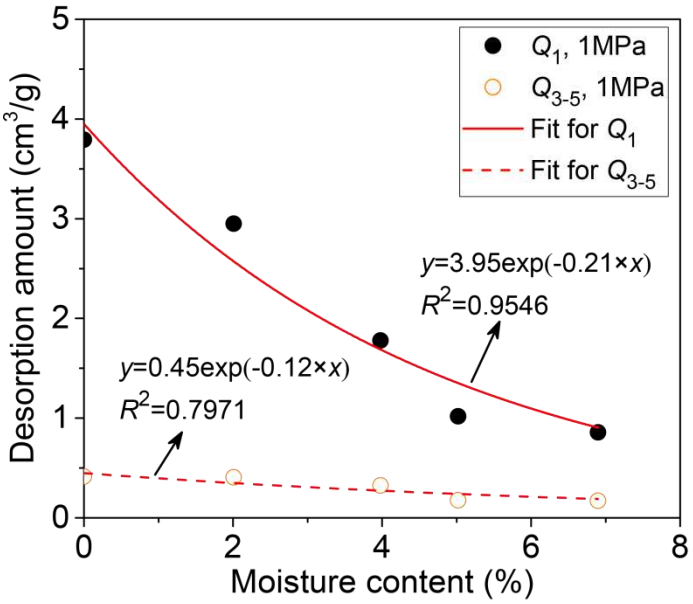

Figure 9 Relationships between Q_1, $Q_{3\text{-}5}$ and moisture content.

As shown in Figure 10, the relationships between methane desorption parameters (V_1, A, K_t) and moisture content at methane pressure of 1 MPa are further studied. Below the studied moisture content, the ultimate desorption amount (A) is decreased by about 0.66 cm^3/g for each 1% increase in moisture content. For the initial desorption rate (V_1), each 1% increase in moisture content can leads to a reduction of about 0.04 cm^3/(g·min). Water molecules have more adsorption advantages than methane molecules and can seize some adsorption spaces of gas molecules (Gensterblum et al. 2013; Gensterblum et al. 2014), thereby reducing the saturated adsorption capacity of moist coal. Furthermore, the reduction in gas adsorption capacity can decreases the concentration gradient of the desorbed gas and gas desorption amount (Liu et al. 2015; Xu et al. 2015), which should be responsible for that the initial desorption rate of low moisture content coal is higher than that of high moisture content coal. Besides, the desorption constant K_t shows a different change trend from the parameters V_1 and A. When the moisture content is less than 3.98%, the parameter K_t decreases slightly, while it reduces significantly at the range of 3.98–6.9%. As analyzed in the sections 4.3.2, this can be attributed to the fact that the constant K_t is mainly related to the fractal dimension D_2 representing the fractal

structural characteristics of larger scale pores.

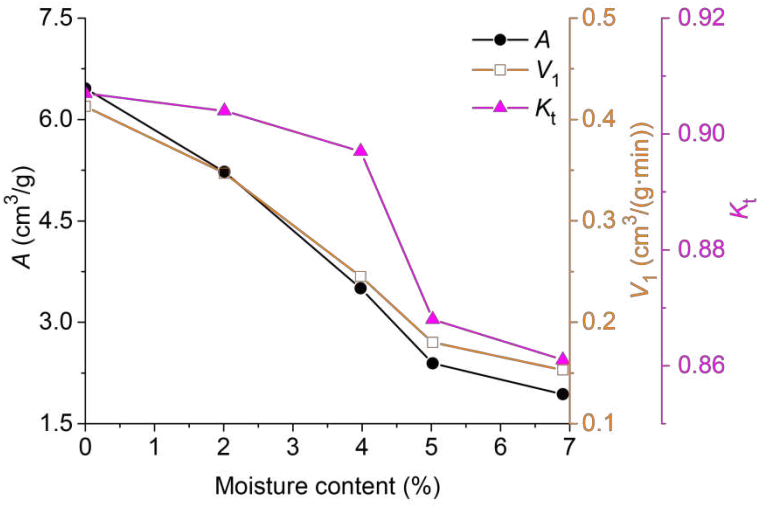

Figure 10 Changes in methane desorption parameters with moisture content.

4.4.2 Relationship between fractal dimension and desorption parameters

Many researchers have indicated that the methane desorption performances of coal is related to pore structure of coal under dry condition (Chen et al. 2017; Liu et al. 2022). In this paper, the Pearson product-moment correlation coefficient (γ) is selected to further analyze the above relationship under moist condition. If the random variable X= { x_1, x_2, x_3, …, x_n}, Y= { y_1, y_2, y_3, …, y_n}, the Pearson correlation coefficient (γ) for the two variables is defined as

$$\gamma = \frac{n\sum x_i y_i - \sum x_i \sum y_i}{\sqrt{n\sum x_i^2 - (\sum x_i)^2}\sqrt{n\sum y_i^2 - (\sum y_i)^2}} \quad (9)$$

where n is the sequence length of the random variable, and γ ranges from -1 to +1. When γ is 0, the two variables are independent; when γ is [-1, 0], the two variables are negatively correlated; and when γ is [0, +1], the two variables are positively correlated. The absolute value of γ is close to 1 suggesting a higher correlation degree.

Combined with the interpolation method, the values of γ between methane desorption parameters (V_1, A, K_t) and fractal dimensions (D_1 and D_2) at gas pressure of 1 MPa are calculated by SPSS software, as shown in Figure 9. The values of γ for the correlations of A and D_1 or V_1 and D_1 are larger

than 0.8, which are slightly higher than that for the correlations of A and D_2 or V_1 and D_2. Conversely, the value of γ for the correlation of D_2 and K_t is 0.780, which is greater than that for the correlation of D_1 and K_t. Therefore, the parameters A and V_1 are more closely related to the fractal dimension D_1, whereas the desorption constant K_t is more dependent on the fractal dimension D_2. This is mainly due to that the fractal dimension D_1 and D_2 represents the surface fractal characteristic of micropores and the structural fractal characteristic of larger scale pores, respectively (Yao et al. 2008; Li et al. 2015).

The methane desorption parameters A and V_1 reflect the ultimate and initial methane desorption capacities, which depend on the methane adsorption amount of coal (Liu et al. 2015). The micropores of coal plays a key role on methane adsorption capacity (An et al. 2013; Song et al. 2020), which provides an explanation for the close relationships between D_1 and A, V_1. Besides, the parameter K_t characterizes the ratio between the gas desorption volume in the macropores and micro-fractures in the first minute after methane gas is relieved (Guo et al. 2014). Chen et al. (2017) further suggested that the methane desorption constant K_t is associated with macropores volumes. Obviously, for both dry coal and water-equilibrated coal, the constant K_t is closely related to D_2 representing fractal dimension of larger scale pores.

Table 6 Correlation coefficients between fractal dimension and desorption parameters.

Variables	A	V_1	K_t
D_1	0.854**	0.847**	0.684**
D_2	0.727**	0.729**	0.780**

Note: ** significance level α= 0.01.

Moreover, in the prevention and control of coal mine gas disasters, many desorption parameters are applied to assess the risk of coal and gas outburst. For example, for the desorption indices Δh_2 and K_1, the outburst critical values of moist coal (Δh_2 = 160 Pa, K_1= 0.4 $cm^3/(g \cdot min^{0.5})$) are provided by some industrial standards (Cheng et al. 2010; Cheng et al. 2016). However, the loss and fluctuation of the adsorbed moisture in low-rank coal will affect the methane adsorption capacity of coal and

415 sequentially lead to the variation in critical values of the desorption indices for outburst prediction. It's
416 necessary to study the quantitative relationship between methane desorption indices and moisture
417 content, and further put forward a reasonable method to determine the critical value of methane
418 desorption indices of in-stiu coal seam. Another revelation is that developing new engineering
419 technologies to reduce the water content of low-rank coal is also necessary to improve gas migration in
420 the development of coalbed methane (CBM) (Guo et al. 2018).

421 **5 Conclusions**

422 (1) Both N_2-SSA and N_2-PV decrease significantly with equilibrium moisture content increases,
423 and the adsorbed moisture has greater influence on coal's micropores with pore diameter less than 10
424 nm. In particular, when the adsorbed moisture content increases to 10.88% that is attained at 98%
425 relatively humidity, the micropores less than 4 nm almost disappear in the DFT-PSDs probably due to
426 the blocking effect of the formed water clusters and capillary water. However, the N_2-SSA of
427 micropores (pore diameter < 10 nm) shows that it can still contributes most sites for gas adsorption on
428 water-equilibrated coal at 98% relatively humidity.

429 (2) The fractal characteristics analyzed by the FHH model shows that, when the equilibrium
430 moisture content is less than 4.74% (corresponding to a *RH* of 43%), D_1 decreases rapidly while D_2
431 shows a slight change, which is mainly due to the water adsorption on coal mainly occurs on the
432 surface of micropores. Whereas, at high equilibrium moisture content (M > 4.74%), the D_2 decreases
433 significantly and D_1 remains at about 2.32 with moisture content increases. The phenomenon can be
434 attributed to the completion of monolayer adsorption of water molecules on micropores, and the
435 pore-filling and pore-blocking effects of the adsorbed water in some pores and throat.

436 (3) The adsorbed moisture has significant negative impact on methane desorption capacity, and

each 1% increase in moisture content can leads to about 11% reduction in Q_1 and about 8% reduction in $Q_{3\text{-}5}$. The analysis on the Pearson's correlation coefficient (γ) shows that, below the studied equilibrium moisture content, the ultimate methane desorption capacity (A) and initial desorption rate (V_1) are closely related to D_1, while the desorption constant K_t mainly depends on D_2.

Declarations

Funding information: This work was supported by the National Natural Science Foundation of China (Grant No. 51804201, 52174230, 51904272), Natural Science Foundation of Hebei Province (Grant No. E2020210081; E2021210128), and the university-level Graduate innovation project (Grant No. YC2021029).

Author's contributions: Chen Ming-yi funding acquisition, Conceptualization, Methodology, Writing-Reviewing and Editing; **Yang Ya-pu** Writing- Original Draft, Data Curation and analysis; **Chen Xiao-yun** Data Curation and analysis; **Tian Fu-chao** Validation, supervision, Investigation; **Sun Wei-li** experiment, Data Curation and analysis; **Yang Yu-meng** Validation, supervision, Investigation; **Zhang Tong-hao** experiment.

Compliance with ethical standards:

Ethical approval Not applicable

Consent to participate Not applicable

Consent to publish Not applicable

Availability of data materials Not applicable

Competing interests The authors declare that they have no conflict of interest.

Reference

Airey E Gas emission from broken coal. An experimental and theoretical investigation. In: International Journal of Rock Mechanics and Mining Sciences & Geomechanics Abstracts,

1968. vol 6. Elsevier, pp 475-494
An FH, Cheng YP, Wu DM, Wang L (2013) The effect of small micropores on methane adsorption of coals from Northern China Adsorption 19:83-90
Andrade P RD, Lemus M R, PÉRez C CE (2011) MODELS OF SORPTION ISOTHERMS FOR FOOD: USES AND LIMITATIONS Vitae 18:325-334
Banerjee B (1988) Spacing of fissuring network and rate of desorption of methane from coals Fuel 67:1584-1586
Busch A, Gensterblum Y (2011) CBM and CO2-ECBM related sorption processes in coal: a review International Journal of Coal Geology 87:49-71
Charrière D, Behra P (2010) Water sorption on coals J Colloid Interface Sci 344:460-467
Chen MY, Cheng YP, Li HR, Wang L, Jin K, Dong J (2018) Impact of inherent moisture on the methane adsorption characteristics of coals with various degrees of metamorphism Journal of Natural Gas Science & Engineering 55:312-320
Chen MY, Cheng YP, Zhou HX, Wang L, Tian FC, Jin K (2017) Effects of Igneous Intrusions on Coal Pore Structure, Methane Desorption and Diffusion within Coal, and Gas Occurrence Environmental & Engineering Geoscience 23:191-207
Chen MY, Yang YP, Gao CH, Cheng YP, Wang JC, Wang N (2020) Investigation of the fractal characteristics of adsorption-pores and their impact on the methane adsorption capacity of various rank coals via N_2 and H_2O adsorption methods Energy Sci Eng doi:10.1002/ese3.727
Chen X, Cheng Y (2015) Influence of the injected water on gas outburst disasters in coal mine Nat Hazards 76:1093-1109
Chen Y, Tang DZ, Xu H, Tao S, Li S, Yang GH, Yu JJ (2015) Pore and fracture characteristics of different rank coals in the eastern margin of the Ordos Basin, China Journal of Natural Gas Science and Engineering 26:1264-1277 doi:10.1016/j.jngse.2015.08.041
Cheng LB, Wang L, Cheng YP, Jin K, Zhao W, Sun LS (2016) Gas desorption index of drill cuttings affected by magmatic sills for predicting outbursts in coal seams Arabian Journal of Geosciences 9 doi:10.1007/s12517-015-2133-8
Cheng YP, Pan ZJ (2020) Reservoir properties of Chinese tectonic coal: A review Fuel 260 doi:10.1016/j.fuel.2019.116350
Cheng YP, Wang HF, Wang L, Zhou HX, Liu HB, Wu DM, Li W (2010) Theories and Engineering Applications on Coal Mine Gas Control. China University of Mining and Technology Press, Xuzhou
Clarkson CR, Bustin RM (2000) Binary gas adsorption/desorption isotherms: effect of moisture and coal composition upon carbon dioxide selectivity over methane International Journal of Coal Geology 42:241-271 doi:https://doi.org/10.1016/S0166-5162(99)00032-4
Do DD, Do HD (2000) A model for water adsorption in activated carbon Carbon 38:767-773
Fu G, Xie XC, Jia QS, Tong WQ, Ge Y (2020) Accidents analysis and prevention of coal and gas outburst: Understanding human errors in accidents Process Saf Environ Protect 134:1-23 doi:10.1016/j.psep.2019.11.026
Gensterblum Y, Busch A, Krooss BM (2014) Molecular concept and experimental evidence of competitive adsorption of H_2O, CO_2 and CH_4 on organic material Fuel 115:581-588
Gensterblum Y, Merkel A, Busch A, Krooss BM (2013) High-pressure CH_4 and CO_2 sorption isotherms as a function of coal maturity and the influence of moisture International Journal of Coal Geology 118:45-57

Guo H, Cheng Y, Wang L, Lu S, Jin K (2015) Experimental study on the effect of moisture on low-rank coal adsorption characteristics Journal of Natural Gas Science & Engineering 24:245-251

Guo HJ et al. (2018) Effect of moisture on the desorption and unsteady-state diffusion properties of gas in low-rank coal Journal of Natural Gas Science and Engineering 57:45-51 doi:10.1016/j.jngse.2018.06.045

Guo J, Kang T, Kang J, Zhao G, Huang Z (2014) Effect of the lump size on methane desorption from anthracite Journal of Natural Gas Science and Engineering 20:337-346

Hong L, Gao DM, Wang JR, Zheng D (2019) The Power Source for Coal and Gas Outburst Journal of Mining Science 55:239-246 doi:10.1134/s1062739119025515

Huang CY, Zhang QY, Yan JM (1979) The study of pore structure analysis by water vapor adsorption-calculation of adsorption thickness and pore size distribution. J Chin Ceram Soc. 7:333-345

Jiang JY, Cheng YP, Mou JH, Jin K, Cui J, Rao ZH (2015) Effect of Water Invasion on Outburst Predictive Index of Low Rank Coals in Dalong Mine Plos One 10:e0132355

Jiang JY, Zhang Q, Cheng YP, Jin K, Zhao W, Guo HJ (2016) Influence of thermal metamorphism on CBM reservoir characteristics of low-rank bituminous coal Journal of Natural Gas Science and Engineering 36:916-930 doi:10.1016/j.jngse.2016.11.030

Kondo S, Ishikawa T, Abe I (2005) Adsorption science Chemical Industry Press, Beijing:84-85

Laxminarayana C, Crosdale PJ (2002) Controls on Methane Sorption Capacity of Indian Coals Aapg Bulletin 86:201-212

Li Y, Yang ZZ, Li XG (2019) Molecular Simulation Study on the Effect of Coal Rank and Moisture on CO_2/CH_4 Competitive Adsorption Energy & Fuels 33:9087-9098

Li Z, Lin B, Gao Y, Cao Z, Cheng Y, Yu J (2015) Fractal analysis of pore characteristics and their impacts on methane adsorption of coals from Northern China International Journal of Oil, Gas and Coal Technology 10:306-324

Liu KQ, Zakharova N, Adeyilola A, Zeng LB (2021) Experimental Study on the Pore Shape Damage of Shale Samples during the Crushing Process Energy & Fuels 35:2183-2191 doi:10.1021/acs.energyfuels.0c03297

Liu P, Liu A, Liu SM, Qi LL (2022) Experimental evaluation of ultrasound treatment induced pore structure and gas desorption behavior alterations of coal FUEL 307:121855 https://doi.org/10.1016/j.fuel.2021.121855

Liu SL, Zhang DF, Lun ZM, Zhao CP, Wang HT (2020) Occurrence of water within different rank coals: a review Energy Sources Part A-Recovery Util Environ Eff doi:10.1080/15567036.2020.1781979

Liu XF, Nie BS (2016) Fractal characteristics of coal samples utilizing image analysis and gas adsorption Fuel 182: 314-322

Liu YW, Feng GZ, Zuo WQ, Liu MJ, Mitri HS (2019) The law and mechanism of dynamic methane diffusion from coal particles under different moisture content Arabian Journal of Geosciences 12 doi:10.1007/s12517-019-4919-6

Liu YW, Zhang JQ, Liu MJ, Li YP (2015) Influence of moisture content on gas diffusion coefficient of coal particles with different metamorphic degree Journal of Safety Science and Technology 11: 12-17

Lowell S, Shields JE, Thomas MA, Thommes M (2004) Characterization of porous solids and powders: surface area, pore size and density vol 16. Springer Science & Business Media, Netherlands

548 Lu S et al. (2021) Gas time-dependent diffusion in pores of deformed coal particles: Model
549 development and analysis Fuel 295:120566 doi:https://doi.org/10.1016/j.fuel.2021.120566
550 Meng JQ, Li SC, Niu JX, Meng HX, Zhong RQ, Zhang LF, Nie BS (2020) Effects of moisture on
551 methane desorption characteristics of the Zhaozhuang coal: experiment and molecular
552 simulation Environ Earth Sci 79 doi:10.1007/s12665-019-8788-9
553 Ni GH, Li S, Rahman S, Xun M, Wang H, Xu YH, Xie HC (2020) Effect of nitric acid on the pore
554 structure and fractal characteristics of coal based on the low-temperature nitrogen adsorption
555 method Powder Technology 367:506-516 doi:10.1016/j.powtec.2020.04.011
556 Nie B, Liu X, Yuan S, Ge B, Jia W, Wang C, Chen X (2016) Sorption charateristics of methane among
557 various rank coals: impact of moisture Adsorption 22:315-325
558 Pan Z, Connell LD, Camilleri M, Connelly L (2010) Effects of matrix moisture on gas diffusion and
559 flow in coal Fuel 89:3207-3217
560 Qi LL, Tang X, Wang ZF, Peng XS (2017) Pore characterization of different types of coal from coal
561 and gas outburst disaster sites using low temperature nitrogen adsorption approach
562 International Journal of Mining Science and Technology 27:371-377
563 doi:10.1016/j.ijmst.2017.01.005
564 Si LL, Wei JP, Xi YJ, Wang HY, Wen ZH, Li B, Zhang HT (2021) The influence of long-time water
565 intrusion on the mineral and pore structure of coal Fuel 290 doi:10.1016/j.fuel.2020.119848
566 Song DY, Ji XF, Li YB, Zhao HT, Song BY, He KK (2020) Heterogeneous development of micropores
567 in medium-high rank coal and its relationship with adsorption capacity International Journal
568 of Coal Geology 226 doi:10.1016/j.coal.2020.103497
569 Švábová M, Weishauptová Z, Přibyl O (2011) Water vapour adsorption on coal Fuel 90:1892-1899
570 Thommes M, Kaneko K, Neimark AV, Olivier JP, Rodriguez-Reinoso F, Rouquerol J, Sing KS (2015)
571 Physisorption of gases, with special reference to the evaluation of surface area and pore size
572 distribution (IUPAC Technical Report) Pure and Applied Chemistry 87:1051-1069
573 Wang BY, Qin Y, Shen J, Wang G (2017) Summarization of geological study on low rank coalbed
574 methane in China Coal Science and Technology 45:170-179
575 Wang CY et al. (2021) Investigation of interactions between oxygen-containing groups and water
576 molecules on coal surfaces using density functional theory Fuel 287
577 doi:10.1016/j.fuel.2020.119556
578 Wang F, Yao YB, Wen ZA, Sun QP, Yuan XH (2020a) Effect of water occurrences on methane
579 adsorption capacity of coal: A comparison between bituminous coal and anthracite coal Fuel
580 266 doi:10.1016/j.fuel.2020.117102
581 Wang FK, Liang YP, Sun ZG, Li L, Li XL (2020b) Determination of the sensitivity index and its
582 critical value for outburst risk prediction: A case study in Fuxiang mine, China Adsorpt Sci
583 Technol 38:502-527 doi:10.1177/0263617420963735
584 Wang K, Zang J, Feng Y, Wu Y (2014a) Effects of moisture on diffusion kinetics in Chinese coals
585 during methane desorption Journal of Natural Gas Science & Engineering 21:1005-1014
586 Wang L, Chen ET, Liu S, Cheng YP, Cheng LB, Chen MY, Guo HJ (2017) Experimental study on the
587 effect of inherent moisture on hard coal adsorption-desorption characteristics Adsorpt-J Int
588 Adsorpt Soc 23:723-742 doi:10.1007/s10450-017-9889-y
589 Wang L, Cheng YP, Liu HY (2014b) An analysis of fatal gas accidents in Chinese coal mines Safety
590 Science 62:107-113 doi:10.1016/j.ssci.2013.08.010
591 Winter K, Janas H (1975) Gas emission characteristics of coal and methods of determining the

592 desorbable gas content by means of desorbometers. In: XIV International Conference of Coal
593 Mine Safety Research, Sept. 22–26: Washington, D.C
594 Xiang JH, Zeng FG, Liang HZ, Li B, Song XX (2014) Molecular simulation of the CH4/CO2/H2O
595 adsorption onto the molecular structure of coal Sci China-Earth Sci 57:1749-1759
596 doi:10.1007/s11430-014-4849-9
597 Xu H, Tang DZ, Zhao JL, Li S, Tao S (2015) A new laboratory method for accurate measurement of the
598 methane diffusion coefficient and its influencing factors in the coal matrix Fuel 158:239-247
599 doi:10.1016/j.fuel.2015.05.046
600 Xue S, Zheng CS, Zheng XL, Jiang BY, Li YB, Wang ZG (2020) Experimental determination of the
601 outburst threshold value of energy strength in coal mines for mining safety Process Saf
602 Environ Protect 138:263-268 doi:10.1016/j.psep.2020.03.034
603 Yao Y, Liu D, Tang D, Tang S, Huang W (2008) Fractal characterization of adsorption-pores of coals
604 from North China: an investigation on CH 4 adsorption capacity of coals International Journal
605 of Coal Geology 73:27-42
606 Yu JL, Tahmasebi A, Han YN, Yin FK, Li XC (2013) A review on water in low rank coals: The
607 existence, interaction with coal structure and effects on coal utilization Fuel Processing
608 Technology 106:9-20 doi:10.1016/j.fuproc.2012.09.051
609 Zhai C, Xiang XW, Xu JZ, Wu SL (2016) The characteristics and main influencing factors affecting
610 coal and gas outbursts in Chinese Pingdingshan mining region Nat Hazards 82:507-530
611 doi:10.1007/s11069-016-2195-2
612 Zhang Y (2008) Geochemical kinetics. Princeton University Press, PRINCETON AND OXFORD
613 Zhang ZG, Cao SG, Li Y, Guo P, Yang HY, Yang T (2018) Effect of moisture content on methane
614 adsorption- and desorption-induced deformation of tectonically deformed coal Adsorpt Sci
615 Technol 36:1648-1668 doi:10.1177/0263617418800905
616 Zou LH, Gong LH, Xu P, Feng GC, Liu HM (2016) Modified GAB model for correlating multilayer
617 adsorption equilibrium data Separation and Purification Technology 161:38-43